AIP | Review of Scientific Instruments

Neutron yield enhancement in laser-induced deuterium-deuterium fusion using a novel shaped target

J. R. Zhao, X. P. Zhang, D. W. Yuan, L. M. Chen, Y. T. Li, C. B. Fu, Y. J. Rhee, F. Li, B. J. Zhu, Yan. F. Li, G. Q. Liao, K. Zhang, B. Han, C. Liu, K. Huang, Y. Ma, Yi. F. Li, J. Xiong, X. G. Huang, S. Z. Fu, J. Q. Zhu, G. Zhao, and J. Zhang

Citation: Review of Scientific Instruments **86**, 063505 (2015); doi: 10.1063/1.4922912
View online: http://dx.doi.org/10.1063/1.4922912
View Table of Contents: http://scitation.aip.org/content/aip/journal/rsi/86/6?ver=pdfcov
Published by the AIP Publishing

REVIEW OF SCIENTIFIC INSTRUMENTS **86**, 063505 (2015)

Neutron yield enhancement in laser-induced deuterium-deuterium fusion using a novel shaped target

J. R. Zhao,[1] X. P. Zhang,[2] D. W. Yuan,[3] L. M. Chen,[1,a)] Y. T. Li,[1] C. B. Fu,[2,b)] Y. J. Rhee,[4] F. Li,[1] B. J. Zhu,[1] Yan. F. Li,[1] G. Q. Liao,[1] K. Zhang,[3] B. Han,[3] C. Liu,[5] K. Huang,[1] Y. Ma,[1] Yi. F. Li,[1] J. Xiong,[6] X. G. Huang,[6] S. Z. Fu,[6] J. Q. Zhu,[7] G. Zhao,[3] and J. Zhang[8]

[1]*Laboratory of Optical Physics, Institute of Physics, CAS, Beijing 100190, China*
[2]*Institute of Nuclear and Particle Physics (INPAC), Department of Physics and Astronomy, Shanghai Jiao Tong University, Shanghai 200240, China*
[3]*Key Laboratory of Optical Astronomy, National Astronomical Observatories, CAS, Beijing 100012, China*
[4]*Nuclear Data Center, Korea Atomic Energy Research Institution, Daejon 305353, Korea*
[5]*Department of Astronomy, Beijing Normal University, Beijing 100875, China*
[6]*Shanghai Institute of Laser Plasma, Shanghai 201800, China*
[7]*National Laboratory on High Power Lasers and Physics, Shanghai 201800, China*
[8]*Laboratory for Laser Plasmas (Ministry of Education) and Department of Physics and Astronomy, Shanghai Jiao Tong University, Shanghai 200240, China*

(Received 3 April 2015; accepted 8 June 2015; published online 29 June 2015)

Neutron yields have direct correlation with the energy of incident deuterons in experiments of laser deuterated target interaction [Roth *et al.*, Phys. Rev. Lett. **110**, 044802 (2013) and Higginson *et al.*, Phys. Plasmas **18**, 100703 (2011)], while deuterated plasma density is also an important parameter. Experiments at the Shenguang II laser facility have produced neutrons with energy of 2.45 MeV using d (d, n) He reaction. Deuterated foil target and K-shaped target were employed to study the influence of plasma density on neutron yields. Neutron yield generated by K-shaped target (nearly 10^6) was two times higher than by foil target because the K-shaped target results in higher density plasma. Interferometry and multi hydro-dynamics simulation confirmed the importance of plasma density for enhancement of neutron yields. © *2015 AIP Publishing LLC.* [http://dx.doi.org/10.1063/1.4922912]

INTRODUCTION

Fast neutron is defined as a neutron with an energy higher than 0.5 eV. The generation of fast neutrons[1,2] arouses great interest for demanding applications, for instance, fusion power plant materials testing,[3] neutron radiography,[4] neutron therapy,[5] and others.[6,7] These applications need a high neutron flux which is possible with spallation sources, nuclear reactors, and conventional accelerators. Unfortunately, these devices are not only significant in space but also extremely expensive to build and maintain.[3] The rapid development of high intensity laser technology offers an alternative with relatively lower cost. Previous work has researched 2.45 MeV neutrons produced by deuterium-deuterium (DD) nuclear reactions[8,9] according to the following reaction channel:

$$\mathrm{D} + \mathrm{D} \rightarrow {}^3\mathrm{He}(0.82\ \mathrm{MeV}) + \mathrm{n}(2.45\ \mathrm{MeV}). \tag{1}$$

Such as 10^7 neutrons are produced by deuterium cluster targets in Coulomb explosion regime,[10] and 10^8 neutrons by bulk deuterated target in Target Normal Sheath Acceleration (TNSA) regime.[11] Time-of-flight (TOF) method is the most common way in neutron detection as the neutron has a characteristic kinetic energy of 2.45 MeV.

While most of these works are focused on improving the energy of incident deuterons since the nuclear cross section increased sharply within the limits of 2 MeV of incident deuteron energy, the density of deuterated plasma is still not negligible either. This issue can be discussed by the definition equation of nuclear reaction cross section as follows:

$$N' = \sigma \cdot I N_s \propto \sigma \cdot \rho, \tag{2}$$

where σ is cross section, N' is the number of fusion events per unit time, I is the number of incident deuterons per unit time which is proportional to the deuterated plasma density ρ, and N_s is the number of target nucleus per unit area. Equation (2) indicates that the contribution for fusion events is derived from two parts. One part is cross section σ which is proportional to the energy of incident deuterons. The other part is product of I and N_s, which is directly related to the deuterated plasma density ρ. Therefore, both the energy of accelerated deuterons and the deuterated plasma density are crucial for neutron generation. When giving a certain laser intensity, the accelerated deuteron kinetic energy which affects the cross section of DD fusion is definite. The number of fusion events N' strongly depends on the deuterated plasma density ρ in this condition.

In this article, we present studies of deuterated targets having different shapes for neutron generation aiming to confirm the significant role of deuterated plasma density for enhancement of neutron yields by DD nuclear reactions. Experimental and theoretical methods are carried out to measure plasma densities of these targets.

EXPERIMENTAL RESULTS AND DISCUSSION

The experiment was performed at Shenguang II laser facility in the National Laboratory on High power Lasers and

a)Electronic mail: lmchen@iphy.ac.cn
b)Electronic mail: cbfu@sjtu.edu.cn

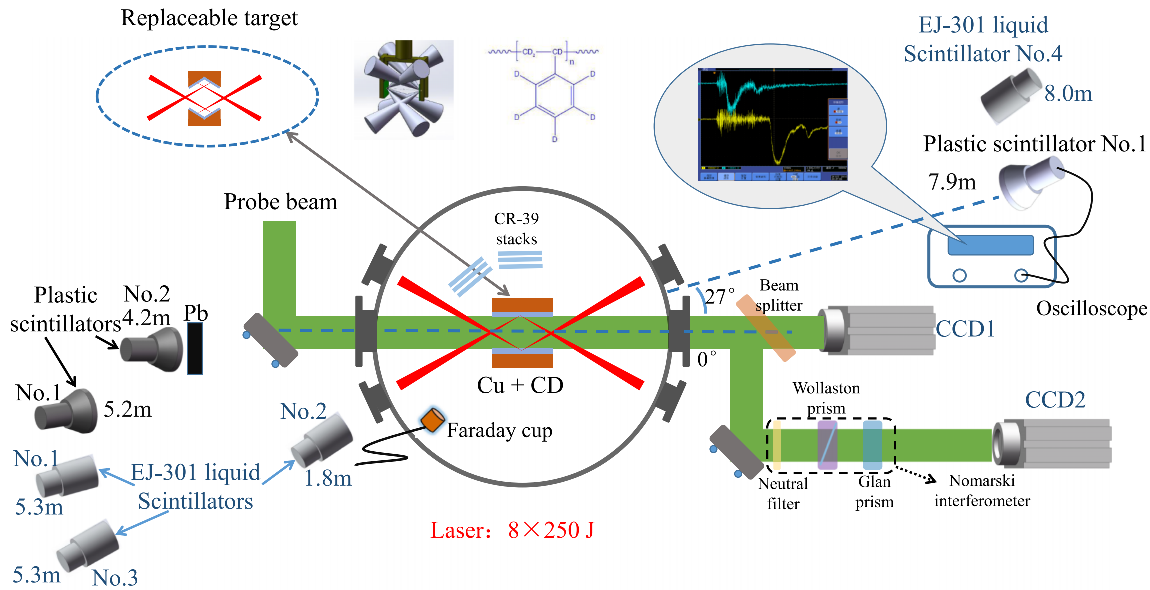

FIG. 1. Layout of the experimental setup. Eight beams of laser are divided into two groups and each group is composed of four laser beams which are focused onto the facing surfaces of the targets at the same time. Two kinds of deuterated targets were employed. One was the 2-side $2\times2\times0.11$ mm^3 foil targets with a separation of 4.5 mm which has a 10 μm deuterated hydrocarbon layer coated on 100 μm copper. The other one was the K-shaped targets with a separation of 3.5 mm which have a 10 or 5 μm thick CD_n layer and an opening angle of 120°. Two plastic and four EJ-301 liquid scintillator detectors were employed to measure the neutron yields by TOF methods. No. 1 plastic detector was located at 5.2 m from the fusion plasma and then was moved to 7.9 m away at the other side of the target chamber, after shot No. 78, while No. 2 plastic detector was located at 4.2 m away with a 20 cm thick lead brick shield in front to decrease the influence of x-ray. The other four liquid detectors were located at 5.3 m, 1.8 m, 5.3 m, and 8.0 m from the plasma interaction area, respectively. The process of plasma expansion and interaction was recorded by the shadowgraph instruments and Nomarski interferometer.

Physics.[12] Eight beams of laser pulses with energy ranging from 200 to 260 J and 1 ns duration can deliver a total energy of more than 2 kJ at 3ω (351 nm) on target. The laser beams are divided into two groups and each group is composed of four laser beams which are focused onto the facing surfaces of the targets at the same time with the focal spot diameter of 150 μm, giving the laser intensity of about 5×10^{15} W $\cdot$ cm^{-2}.

The experimental setup was shown in Fig. 1. Two kinds of deuterated targets were employed. One was the 2-side $2\times2\times0.11$ mm^3 foil targets with a separation of 4.5 mm which have a 10 μm deuterated hydrocarbon (CD_n, the ratio of carbon to deuterium in the CD_n molecules was 1:1.3) layer coated on 100 μm copper. The other one was the K-shaped targets with a separation of 3.5 mm which have a 10 or 5 μm thick CD_n layer and an opening angle of 120°. Both of the targets have two opposite sides. Each laser group consists of four laser pulses which shine on one surface of the target. This kind of shooting pattern was pictured as there are only two laser beams on one side in Fig. 1, because the other two laser beams are concealed in the picture. Another laser pulse (the ninth pulse) with duration of 70 ps and wavelength of 526 nm (2ω) was arranged as a probe beam. By changing the delay time between the probe beams and the main laser pulses, the process of plasma expansion and interaction was recorded by the shadowgraph instruments and Nomarski interferometer.

Two plastic and four EJ-301 liquid scintillator detectors were employed to measure the neutron yields from the DD fusion reactions by TOF methods. As shown in Table I, the plastic scintillator has a larger active area to collect neutrons with a size of $\pi\times16\times16$ cm^2. The liquid scintillator detectors are more sensitive to neutrons with a comparable size of $\pi\times6.3\times6.3$ cm^2. No. 1 plastic detector was located at 5.2 m from the fusion plasma and then was moved to 7.9 m away at the other side of the target chamber, after shot No. 78, to make sure the signal that we have achieved was 2.45 MeV neutron considering longer time of flight, while No. 2 plastic detector was located at 4.2 m away with a 20 cm thick lead brick shield in front to decrease the influence of x-ray. The other four liquid detectors were located at 5.3 m, 1.8 m, 5.3 m, and 8.0 m from the plasma interaction area, respectively. All of the neutron TOF signals were recorded by oscilloscopes with bandwidth of 1 GHz. Two stacks three layers of CR-39 detectors were placed 44 cm away from target to diagnose the absolute neutron number.

High density plasma with numerous energetic deuterium ions was produced by laser focused onto the target, then expanded towards the opposite target, and DD nuclear reaction occurred. Figure 2 shows the sample neutron results from

TABLE I. Comparison of the main features of the neutron detectors.

Title	Plastic scintillator		Liquid scintillator			
Detector no.	1	2	1	2	3	4
Diameter (cm)	32	32	12.7	12.7	12.7	12.7
Solid angle (mrad)	3	4.6	0.4	3.8	0.4	0.2
Distance (m)	5.2	4.2	5.3	1.8	5.3	8.0
nTOF (ns)	239	193	244	83	244	368
High voltage(V)	750	750	1625	1800	1650	1850
Remarks	Large active area		Sensitive to neutron			

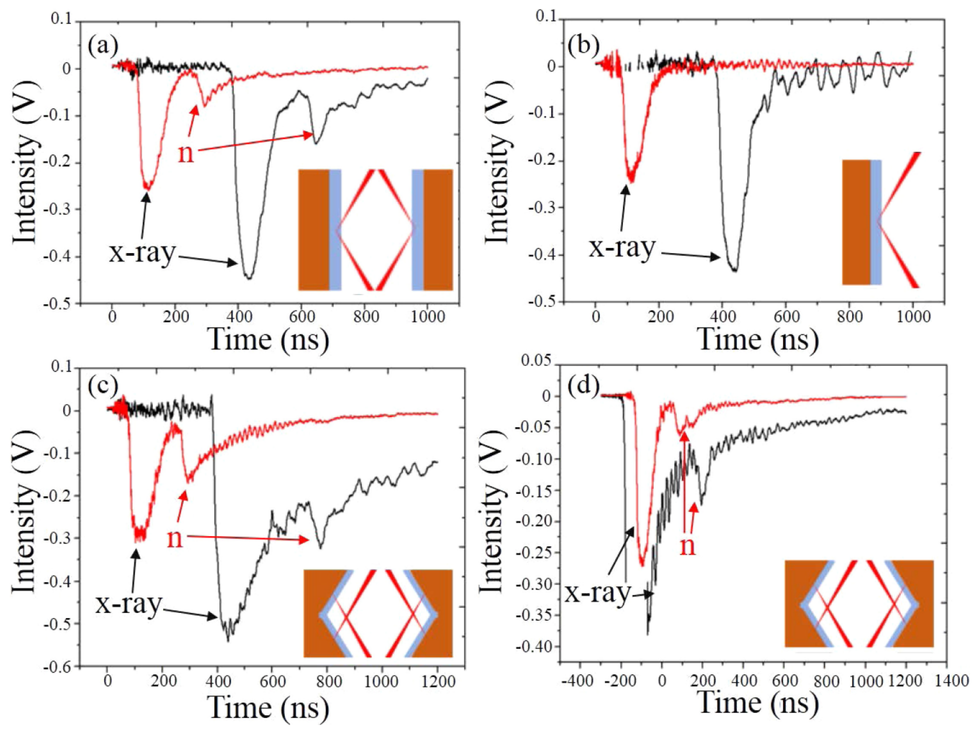

FIG. 2. Neutron TOF results from two plastic detectors, the black line and the red line represent data from detector No. 1 and detector No. 2, respectively. (a) 10 μm thick two-side CD_n foil target irradiated by eight laser beams. (b) 10 μm thick one-side CD_n foil target irradiated by four laser beams. (c) 10 μm thick two-side CD_n K-shaped target irradiated by eight laser beams. (d) 5 μm thick two-side CD_n K-shaped target irradiated by eight laser beams. The presence of initial x-ray and 2.45 MeV neutron is clearly visible in these spectra.

the plastic detectors. As we mentioned before, two groups of lasers (eight beams in all) are used. Figure 2(a) shows TOF signals from the 10 μm thick two-side CD_n foil target irradiated by two groups of lasers. The initial x-ray peak was followed by the 2.45 MeV neutron signal (which have a flight time of 46 $\text{ns} \cdot \text{m}^{-1}$). As the velocity of x-ray is fast enough, it is reasonable to consider that the x-ray is detected at the same time of laser interacting with target, so we regard the starting time of x-ray signal as the zero time. The 2.45 MeV neutron signal was appeared at ~240 ns and 190 ns relative to the falling edge of x-ray signal in Fig. 2(a). Since the signal transmission line of the detector No. 1 is 50 m longer than that of the detector No. 2, these two TOF lines generated the desynchronization of 250 ns. Figure 2(b) shows TOF signals of just an x-ray peak without neutron signal when one group of laser beams irradiated 10 μm thick one-side CD_n foil target. This is a strong evidence that neutrons were produced by two-sides deuterated hot plasma collided with each other or one-side deuterated hot plasma expanded to the other side of the cold target and collided with it.[13] Therefore, both the density of deuterated plasma and the initial thickness of the deuterated target are considerable parameters in this experiment. As we know, neutron yields are proportional to the area of neutron signal, Figure 2(c) shows dramatic increase of neutron yields when two group of laser beams irradiated 10 μm thick two-side CD_n K-shaped target. K-shaped target was employed to increase the density of deuterated plasma.[14] Figure 2(d) shows almost two times lower neutron yields than Figure 2(c) when 5 μm thick two-side CD_n K-shaped target was used. Results from the four EJ-301 liquid scintillator detectors are not discussed in this article because of the foil targets' data loss. The only achieved K-shaped target data could not support the theory of neutron yields enhancement by changing the deuterated plasma density.

To calculate the absolute neutron yields, a DD neutron tube (10^6 n/s) and a ^{137}Cs γ-ray source were used as criterion. According to the measured data, we acquired that the average signal area of one neutron is 170 $\text{mV} \cdot \text{ns}$. Thus, the integrated area of neutron signal in each shot results in the number of neutrons detected on a detector. Then, we took the Geant4 Monte Carlo code[15] to simulate the process of neutron-to-photon to obtain the detection efficiency of neutron detectors. Detailed calibration results were discussed in Ref. 13. The total neutron yield is obtained after considering the solid angle of each neutron detector. Figure 3 shows the neutron yields at different shot numbers. When using the 10 μm thick CD_n foil target, approximately 4×10^5 neutron was produced. More than twice enhancement of neutron yields was produced when changing the target by a 10 μm thick CD_n K-shaped target of which the neutron yield reached the maximum value up to 10^6. That means K-shaped target was more appropriate to produce neutron than foil target in same laser conditions. When replacing the target by a 5 μm thick CD_n K-shaped target, the neutron yields sharply dropped to 3×10^5. This clearly demonstrates that neutron yields are related to the colliding efficiency of deuterated ions, which is directly proportional to the density of deuterated plasma. These results of neutron yields were confirmed by the CR-39 stacks detectors as there were no significant neutron tracks. Because the intrinsic noise density of CR-39 was several hundreds per cm^2,[16,17] neutron tracks cannot be clearly identified when neutron yields were lower than 10^6 in our experiment condition.

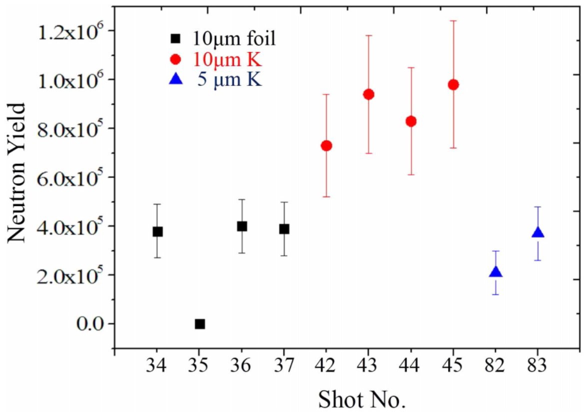

FIG. 3. Neutron yields at different shot numbers. Black square, red circle, and blue triangle in the diagram represent results from 10 μm thick CD_n foil target, 10 μm thick CD_n K-shaped target, and 5 μm thick CD_n K-shaped target, respectively.

To achieve the plasma density of different kinds of targets, interferograms were obtained by using the Nomarski interferometer and were analyzed by means of Abel inversion. Figures 4(a) and 4(b) show interferograms of 10 μm thick CD_n foil target at 1 ns after irradiation and K-shaped target at 2 ns, respectively. The displacement of interferometric fringes in Fig. 4(a) indicates density fluctuation at that area. When plasma density is higher than critical density ~4×10^{21} cm^{-3}, the probe beam cannot penetrate the plasma. So the overcritical plasma region is presented in black and no fringes are shown. There is a distinct opaque plasma jet at the center of Fig. 4(b). Figure 4(c) shows the plasma number density distribution of 10 μm CD_n foil target at 1 ns, corresponding to Fig. 4(a). The white area inside the figure indicates plasma density higher than critical density. This overdense region was produced by the expansion of the initial target body and target holder. The red area at the middle of the figure indicates plasma density is lower than 3×10^{19} cm^{-3} which is most effective in DD nuclear reactions. Figure 4(d) shows the density distribution of the 10 μm thick CD_n K-shaped target at 2 ns, corresponding to Fig. 4(b). Marked plasma jet with density higher than critical density was acquired at the middle of the figure, represented as the dotted arrow. Obviously, the plasma density achieved from the K-shaped target is much higher than that from foil target. Combining it with Eq. (2), the highest yield of neutrons of the K-shaped target is well explained because the K-shaped target has the highest deuterated plasma density. Figures 4(e) and 4(f) show the multi hydro-dynamics simulation results of 10 μm thick CD_n foil target and 10 μm thick CD_n K-shaped target at 2 ns, respectively. The plasma mass density is presented in the figure which is interpreted as the sum densities of electrons, deuterium ions, cupric ions, and some other species. Comparing the two figures, K-shaped target generates an overdense region along the horizontal axis in the middle of the figure due to the overlap of the two plasma streaming from both the upper and the lower parts of

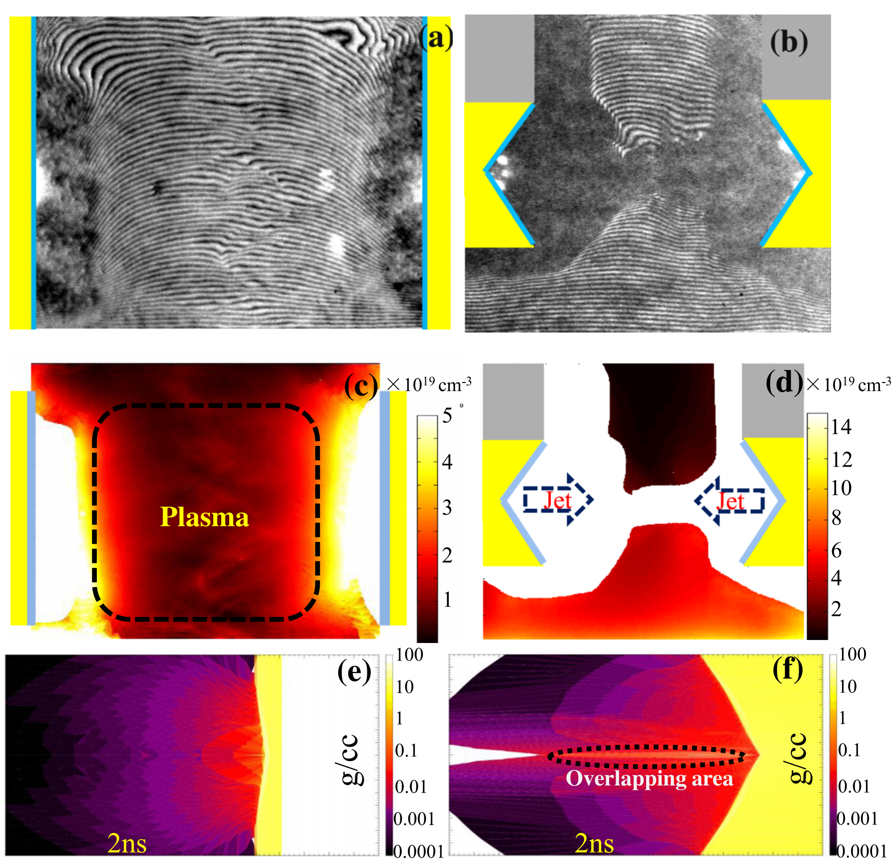

FIG. 4. Interferograms (a) and (b), plasma number density distribution (c) and (d), and plasma mass density distribution (e) and (f) of 10 μm thick CD_n targets. Interferograms of foil target (a) at 1 ns and K-shaped target (b) at 2 ns after irradiation. Experimental plasma density distribution of foil target (c) and K-shaped target (d) corresponding to (a) and (b), respectively. Plasma mass density distribution of foil target (e) and K-shaped target (f) at 2 ns by multi hydro-dynamics simulation.

the K-shaped target having an opening angle of 120°. Since there is no collision cross section module embedded in the simulation code, the process of extrusion and collision of the plasma cannot be reflected in this figure. However, the noticeable overlap of the two plasma streaming in Figure 4(f), to some extent, can explain why K-shaped target produced higher density plasma than foil target.

CONCLUSION

In conclusion, we have presented experimental studies in which eight-beam-laser pulses irradiated deuterated targets producing overdense deuterated plasma and $\sim 1 \times 10^6$ fusion neutrons per operation shot. K-shaped targets were employed to increase the plasma density, which is directly correlated to the neutron yields. Results from K-shaped target show distinct density enhancement compared with foil target. Ultimately, more than two times as many neutrons were achieved by using the K-shaped target than was the case with the foil target. Several orders of magnitude improvement of neutron yields could be acquired when increasing both plasma temperature and plasma density in future work.

ACKNOWLEDGMENTS

This work is supported by the National Basic Research Program of China (No. 2013CBA01500), the National Key Scientific Instrument and Equipment Development Project (No. 2012YQ120047), the National Natural Science Foundation of China (Nos. 11334013, 11135012, and 11375262), the Key Program of the Chinese Academy of Science (KGZD-EW-T05), the Doctoral Fund of Ministry of Education of China (No. 20120073110065), and the Shanghai Municipal Science and Technical Commission (No. 11DZ2260700). We gratefully acknowledge the staff at SG-II laser facility. We also want to thank Dr. Leli Wang at Beijing Normal University for CR-39 corrosion work and Dr. Dazhang Li at Institute of High Energy Physics for extensive discussions.

[1] M. Roth, D. Jung, K. Falk, N. Guler, O. Deppert, M. Devlin, A. Favalli, J. Fernandez, D. Gautier, M. Geissel, R. Haight, C. E. Hamilton, B. M. Hegelich, R. P. Johnson, F. Merrill, G. Schaumann, and K. Schoenberg, Phys. Rev. Lett. **110**, 044802 (2013).
[2] D. P. Higginson, J. M. McNaney, D. C. Swift, G. M. Petrov, J. Davis, J. A. Frenje, L. C. Jarrott, R. Kodama, K. L. Lancaster, A. J. Mackinnon, H. Nakamura, P. K. Patel, G. Tynan, and F. N. Beg, Phys. Plasmas **18**, 100703 (2011).
[3] L. J. Perkins, B. G. Logan, M. D. Rosen, M. D. Perry, T. Diaz de la Rubia, N. M. Ghoniem, T. Ditmire, P. T. Springer, and S. C. Wilks, Nucl. Fusion **40**(1), 301 (2000).
[4] R. Loveman, J. Bendahan, T. Gozani, and J. Stevenson, Nucl. Instrum. Methods Phys. Res., Sect. B **99**, 765 (1995).
[5] L. H. Gray and J. Read, Nature **3845**, 53 (1943).
[6] A. Buffler, Radiat. Phys. Chem. **71**, 853 (2004).
[7] K. L. Lancaster, S. Karsch, H. Habara, F. N. Beg, E. L. Clark, R. Freeman, M. H. Key, J. A. King, R. Kodama, K. Krushelnick, K. W. D. Ledingham, P. McKenna, C. D. Murphy, P. A. Norreys, R. Stephens, C. Stoeckl, Y. Toyama, M. S. Wei, and M. Zepf, Phys. Plasmas **11**, 3404 (2004).
[8] T. Ditmire, J. Zweiback, V. P. Yanovsky, T. E. Cowan, G. Hays, and K. B. Wharton, Nature **398**, 489 (1999).
[9] J. Zweiback, R. A. Smith, T. E. Cowan, G. Hays, K. B. Wharton, V. P. Yanovsky, and T. Ditmire, Phys. Rev. Lett. **84**, 2634 (2000).
[10] W. Bang, M. Barbui, A. Bonasera, G. Dyer, H. J. Quevedo, K. Hagel, K. Schmidt, F. Consoli, R. De Angelis, P. Andreoli, E. Gaul, A. C. Bernstein, M. Donovan, M. Barbarino, S. Kimura, M. Mazzocco, J. Sura, J. B. Natowitz, and T. Ditmire, Phys. Rev. Lett. **111**, 055002 (2013).
[11] L. Torrisi, Molecules **19**, 17052 (2014).
[12] X. Liu, Y. T. Li, Y. Zhang, J. Y. Zhong, W. D. Zheng, Q. L. Dong, M. Chen, G. Zhao, Y. Sakawa, T. Morita, Y. Kuramitsu, T. N. Kato, L. M. Chen, X. Lu, J. L. Ma, W. M. Wang, Z. M. Sheng, H. Takabe, Y. J. Rhee, Y. K. Ding, S. E. Jiang, S. Y. Liu, J. Q. Zhu, and J. Zhang, New J. Phys. **13**, 093001 (2011).
[13] X. P. Zhang, J. R. Zhao, D. W. Yuan, C. B. Fu, Y. T. Li, L. M. Chen, Y. J. Rhee, and J. Zhang, "Studies of D (D, n)^3 He reactions induced by laser plasma collision," Chin. Sci. Bull. (unpublished).
[14] D. W. Yuan, Y. T. Li, L. N. Su, G. Q. Liao, C. L. Yin, B. J. Zhu, and J. Zhang, Sci. China: Phys., Mech. Astron. **56**, 2381 (2013).
[15] S. Agostinelli, J. Allison, K. Amako, J. Apostolakis, H. Araujo, P. Arce, M. Asai, D. Axen, S. Banerjee, and G. Barrand, Nucl. Instrum. Methods Phys. Res., Sect. A **506**, 250 (2003).
[16] W. Bang, H. J. Quevedo, G. Dyer, J. Rougk, I. Kim, M. McCormick, A. C. Bernstein, and T. Ditmire, Rev. Sci. Instrum. **83**, 063504 (2012).
[17] J. A. Frenje, C. K. Li, F. H. Seguin, D. G. Hicks, S. Kurebayashi, R. D. Petrasso, S. Roberts, V. Y. Glebov, D. D. Meyerhofer, T. C. Sangster, J. M. Soures, C. Stoeckl, C. Chiritescu, G. J. Schmid, and R. A. Lerche, Rev. Sci. Instrum. **73**, 2597 (2002).